RORγt+ innate lymphoid cells regulate intestinal homeostasis by integrating negative signals from the symbiotic microbiota

Gerard Eberl, Shinichiro Sawa, Matthias Lochner, Naoko Satoh-Takayama, Sophie Dulauroy, Marion Berard, Melanie Kleinschek, Daniel J Cua, James P. Di Santo

RORγt$^+$ innate lymphoid cells regulate intestinal homeostasis by integrating negative signals from the symbiotic microbiota

Shinichiro Sawa[1,2], Matthias Lochner[1,2,3], Naoko Satoh-Takayama[4,5], Sophie Dulauroy[1,2], Marion Bérard [6], Melanie Kleinschek[7], Daniel Cua[7], James P. Di Santo[4,5] and Gérard Eberl[1,2]

[1]Institut Pasteur, Lymphoid Tissue Development Unit, 75724 Paris, France

[2]CNRS, URA1961, 75724 Paris, France

[3]Institute of Infection Immunology, TWINCORE, Centre for Experimental and Clinical Infection Research; a joint venture between the Medical School Hannover (MHH) and the Helmholtz Centre for Infection Research (HZI), Hannover, Germany

[4]Institut Pasteur, Innate Immunity Unit, 75724 Paris, France

[5]Inserm, U668, 75724 Paris, France

[6]Institut Pasteur, Animalerie Centrale, 25 rue du Dr Roux, 75724 Paris, France

[7]Merck Research Laboratories, DNAX Discovery Research, 94304 Palo Alto, USA

Correspondence should be addressed to G.E. (gerard.eberl@pasteur.fr)

ABSTRACT

RORγt$^+$ lymphoid cells are involved in containment of the large intestinal microbiota and defense against pathogens through the production of IL-17 and IL-22. They include adaptive T_H17 cells, as well as innate lymphoid cells (ILCs), such as lymphoid tissue inducer (LTi) cells and IL-22-producing NKp46$^+$ cells. We find that, in contrast to T_H17 cells, both types of RORγt$^+$ ILCs constitutively produced most of the intestinal IL-22, and that symbiotic microbiota repressed this function through epithelial expression of IL-25. This function was increased in the absence of adaptive immunity and fully restored and required upon epithelial damage, demonstrating a central role for RORγt$^+$ ILCs in intestinal homeostasis. Our data reveal a finely tuned equilibrium between intestinal symbionts, adaptive immunity and RORγt$^+$ ILCs.

INTRODUCTION

The mammalian intestine hosts a large microbiota that includes an estimated 10^{14} bacteria and 100 to 1000 individual species [1]. In order to contain this microbiota and fight breaches by invading microbes, the intestinal immune system deploys a complex network of lymphoid tissues and cells [2,3]. Part of this system is programmed to develop during ontogeny, such as mesenteric lymph nodes and Peyer's patches, and part of it is induced by the microbiota, such as the formation of numerous isolated lymphoid follicles (ILFs) from pre-formed cryptopatches, and the recruitment of various subsets of intestinal lymphocytes [4]. An equilibrium is established between the microbiota and the immune system that is fundamental to intestinal homeostasis [5,6]. Perturbation of homeostasis leads to inflammatory disease characterized by immune attack on microbial symbionts and tissue destruction, a scenario unfolding during inflammatory bowel disease (IBD), or on the contrary, to low reactivity of the intestinal immune system and increased susceptibility to pathogens [7].

A number of cytokines play a key role in intestinal homeostasis. Whereas pro-inflammatory cytokines, such as interferon-γ (IFN-γ), IL-17 and tumor necrosis factor (TNF), promote the elimination of intruding microbes, the anti-inflammatory cytokines IL-10 and TGF-β limit the amplitude of inflammation and favor the production and secretion of IgA, essential to mucosal immunity [2,3]. Another member of the IL-10 cytokine family, IL-22, has been shown to directly induce epithelial defense through the expression of anti-microbial peptides, such as β-defensins [8], S100A7 (psoriasin), S100A8 (calgranulin A), S100A9 (calgranulin B) [9], RegIIIβ and RegIIIγ [10]. IL-22 plays a critical role in defense against attaching and effacing bacterial pathogens in the intestine, such as *Citrobacter rodentium* [10,11], Gram-negative bacteria in the lung, such as *Klebsiella pneumoniae* [12] and against the fungi *Candida albicans* [13]. IL-22 also induces anti-apoptotic molecules, such as Bcl-2 family members, through the activation of STAT3 (ref. 14), and as a possible consequence, protects colon and hepatocytes from acute inflammation [15,16].

IL-22 is efficiently induced by IL-23 [17] and produced at high amounts by $CD4^+$ T_H17 cells [18,19], but also by other subsets of T helper cells [20], $CD8^+$ T cells, γδ T cells [18] and NK cells [16,21]. Recently, it was revealed that a subset of mucosal innate lymphoid cells (ILCs) expressing the pan-NK markers NKp46 in mouse and NKp44 in human, expressed IL-22 [22-27], and mice lacking these IL-22^+ NKp46^+ cells showed increased susceptibility to *C. rodentium* infection [23]. It was also shown that $CD4^+$ lineage-negative (Lin^-) cells in the spleen, a phenotype reminiscent of lymphoid tissue inducer (LTi) cells required for the development of

secondary lymphoid tissues [28] and isolated lymphoid follicles (ILFs) in the intestine [29], express IL-22 [11,30,31]. Common to T_H17 cells [32], IL-22$^+$ NKp46$^+$ or NKp44$^+$ cells, and LTi cells [33], is the expression of the nuclear hormone receptor RORγt, and the requirement for RORγt during their development. Common also to T_H17 cells [34] and a subset of IL-22$^+$ NKp46$^+$ cells, but not to LTi cells [25,35], is a development induced by intestinal symbiotic microbiota.

Using RORγt-EGFP reporter mice [36], we now show that RORγt$^+$ ILCs, including IL-22$^+$ NKp46$^+$ cells and LTi cells, produced most of the intestinal IL-22. In contrast to T cells, this expression of IL-22 was constitutive, highest before weaning and independent of microbial colonization. However, microbiota repressed the production of IL-22 by RORγt$^+$ ILCs through the expression of IL-25 in epithelial cells, whereas the role of IL-23 was minimal. The IL-22-producing activity and numbers of RORγt$^+$ ILCs was increased in the absence of adaptive immunity and RORγt$^+$ T cells, presumably as a consequence of larger niche availability. Furthermore, upon epithelial damage and consequent intestinal inflammation, RORγt$^+$ ILCs regained full activity and were required for survival and recovery. Collectively, our data demonstrate that IL-22 production by RORγt$^+$ ILCs is programmed, and regulated by microbiota and adaptive immunity, presumably to maintain a necessary equilibrium between microbiota and the different forces of immunity.

RESULTS

RORγt$^+$ ILCs are the major source of intestinal IL-22

The nuclear hormone receptor RORγt is expressed by T cells [32,36] and NKp46$^+$ or NKp44$^+$ cells that produce IL-22 [23-26]. To determine the proportion of intestinal IL-22$^+$ cells among RORγt$^+$ cells, we examined BAC-transgenic *Rorc(γt)-Gfp*^{TG} mice [36]. We found that in fetuses (E15), pre-weaned (2 weeks) and adult mice (8 weeks), most IL-22$^+$ cells expressed RORγt (**Fig. 1a**). The vast majority of IL-22$^+$ cells (99%, 80% and 83%, respectively, at these ages) did not express CD3ε, and IL-22$^+$ CD4$^+$ T cells that include T_H17 cells represented only 11% of the total IL-22$^+$ cells in the adult. RAG-deficient mice that lack T cells did not show a significant decrease in the expression of *Il22* in the small intestine, whereas RORγt- or RAG/RORγt-double deficient mice, which lack RORγt$^+$ cells, showed no detectable expression of *Il22* (**Fig. 1b**) and a consequent decreased expression of *Reg3b* and *Reg3g* (**Fig. 1c**). These results demonstrate that most intestinal IL-22 is produced by RORγt$^+$ ILCs.

In the fetus, RORγt$^+$ ILCs consist mainly of CD4$^+$ LTi (LTi_4) cells [33], whereas after birth, the pool of CD4$^-$ RORγt$^+$ ILCs, including CD4$^-$ LTi (LTi_0) cells [37], expanded, and NKp46$^+$ RORγt$^+$ ILCs were generated (**Fig. 1d**). RORγt$^+$ ILCs were found mostly in the intestinal lamina propria (**Supplementary Fig. 1a**) and did not include B cells, dendritic cells (DCs) or cells of the monocyte/macrophage lineage (**Supplementary Fig. 1b**). The expression of IL-22 by RORγt$^+$ ILCs was highest in fetal and pre-weaned animals, and substantially decreased thereafter (**Fig. 2a**). A similar expression profile was found in LTi_4 cells for IL-17 (**Fig. 2b**), co-expressed by a sizeable fraction of IL-22$^+$ cells (**Supplementary Fig. 2a** and **b**), and to a lesser degree in all RORγt$^+$ ILCs for genes involved in lymphoid tissue development, such as *Lta* (coding for lymphotoxin α) (**Fig. 2c**) and *Tnfsf11* (coding for Trance) [38] (**Supplementary Fig. 2c**). The expression of *Ifng* transcripts, produced by the NK1.1$^+$ subset of RORγt$^+$ NKp46$^+$ cells [23], was also decreased after weaning (**Fig. 2c**). Finally, the remaining CD4$^-$ NKp46$^-$ RORγt$^+$ ILCs (**Fig. 1d**), which include c-kit^{hi} LTi_0 cells and poorly characterized c-kit^{low} RORγt$^+$ ILCs expressing IFNγ, also showed decreased expression of IL-22, IL-17, *Lta* and *Ifng* after weaning (**Supplementary Fig. 3**).

Microbiota represses IL-22 production by RORγt$^+$ ILCs

Microbiota induces the generation of RORγt$^+$ T_H17 cells [34] and of the NK1.1$^{lo/-}$ subset of intestinal NKp46$^+$ RORγt$^+$ ILCs [23,25]. However, our data now show that LTi cells constitutively expressed IL-22 in the sterile environment of the fetus, and that expression of IL-22 by RORγt$^+$ ILCs was decreased after weaning. As microbial colonization of the intestine is vastly increased after weaning, we hypothesized that symbiotic microbiota is repressing the activity of RORγt$^+$ ILCs. First, and in contrast to RORγt$^+$ T cells, the number of RORγt$^+$ ILCs remained unchanged in germfree or antibiotic-treated *Rorc(γt)-Gfp*^{TG} mice (**Fig. 3a**), in accordance with data obtained for LTi cells [35]. These observations were valid for both LTi cells and NKp46$^+$ RORγt$^+$ ILCs, the latter including varying proportions of NK1.1^{hi} cells that are reported not to be affected by microbiota [23]. Furthermore, production of IL-22 by RORγt$^+$ ILCs was de-repressed in adult germfree and antibiotic-treated mice (**Fig. 3b**) to concentrations reached in fetal and pre-weaned mice (**Fig. 2a**). This microbiota-induced repression appeared specific for IL-22 production and not operative on IL-17 production (**Fig. 3c**).

Microbiota represses RORγt$^+$ ILCs through IL-25

It has been reported that the differentiation of T_H17 cells in the colon of BALB/c mice is inhibited by IL-25 induced by the microbiota [39]. In accordance with these data, we found that the expression of *Il25* in the ileal epithelium of germfree mice was markedly decreased as compared to SPF mice (**Fig. 4a**). In addition, in SPF mice, expression of *Il25* by epithelial cells increased with age, presumably as a result of microbial colonization of the intestine. As this *Il25* expression pattern inversely correlated with the production of IL-22 by RORγt$^+$ ILCs, we assessed the activity of RORγt$^+$ ILCs in IL-25-deficient mice. Whereas the number of RORγt$^+$ ILCs increased marginally in the absence of IL-25 (**Fig. 4b**), the production of IL-22 was significantly increased (**Fig. 4c**), but not to amounts reached in germfree or pre-weaned mice (**Fig. 2a** and **3b**). Administration of IL-25 to *Rorc(γt)-Gfp*^{TG} mice efficiently repressed IL-22 production by RORγt$^+$ ILCs (**Fig. 4d**) and, as a probable consequence, inhibited the expression of *Reg3b* and *Reg3g* by epithelial cells (**Fig. 4e**).

The inhibitory effect of IL-25 on RORγt$^+$ ILCs was indirect as RORγt$^+$ ILCs did not express IL-25R (or IL-17BR) (**Fig. 4f**). In contrast, IL-17BR was expressed by RORγt$^-$ ILCs, recently reported to expand and produce IL-13 upon administration of IL-25 in mice and involved in early immunity against intestinal helminthes [40,41]. IL-17RB was also expressed by CD11c$^+$ DCs in cryptopatches, which are clusters of LTi cells [29]. When IL-17BR$^+$ DCs were

added to cultures of RORγt$^+$ ILCs, IL-25 efficiently repressed the production of IL-22 by RORγt$^+$ ILCs (**Fig. 4g**), demonstrating that IL-17RB$^+$ ILCs or DCs could mediate the inhibitory effect of IL-25 on the activity of RORγt$^+$ ILC. Transwell analysis showed that this inhibitory effect required contact between IL-17BR$^+$ DCs and RORγt$^+$ ILCs **(Fig. 4h)**, in accordance with our recent data showing that in CCR6-deficient mice that develop abnormal cryptopatches, the expression of IL-22 by RORγt$^+$ ILC is increased [11,30,31].

IL-23 is a potent inducer of IL-22 [17-19], and may be modulated by microbiota and IL-25. We therefore assessed whether the increased IL-22 production by RORγt$^+$ ILCs in germfree mice was a consequence of increased IL-23 in intestinal tissues. However, as might be expected, the expression of *Il23* was decreased in germfree mice (**Supplementary Fig. 4a**). Furthermore, the absence of IL-25 or administration of IL-25 had no effect on the expression of *Il23* and IL-23 protein (**Supplementary Fig. 4b**), excluding that IL-25 regulated the activity of RORγt$^+$ ILCs through IL-23, and the expression of *Il23r* by RORγt$^+$ ILCs was not modulated by IL-25 (**Supplementary Fig. 4c**). Finally, in p19-deficient mice that lack IL-23 **(Supplementary Fig. 4d)**, or in wild-type mice treated with neutralizing antibody specific for IL-23R **(Supplementary Fig. 4e)**, the production of IL-22 by RORγt$^+$ ILCs and its repression by IL-25 were unaffected. Together, these data show that IL-23 is not necessary for or involved in the regulation of IL-22 production by RORγt$^+$ ILCs.

Adaptive immunity represses the activity of RORγt$^+$ ILCs

Both RORγt$^+$ T cells [18,19] and RORγt$^+$ ILCs produce IL-22. These two cell types might therefore compete for regulating factors and thereby mutually regulate their activity. In accordance with this view, the production of IL-22 by RORγt$^+$ ILCs was markedly enhanced in RAG-2-deficient mice (**Fig. 5a**), and the absolute numbers of RORγt$^+$ ILCs was increased 4-fold (**Fig. 5b**). As pointed out earlier, de-repression of the IL-22 production by RORγt$^+$ ILCs was only partial in IL-25-deficient mice as compared to germfree mice (**Fig. 4c** and **3b**). An additional level of repression is thus provided by adaptive immunity, possibly through RORγt$^+$ T cells that compete for a cytokine niche also occupied by RORγt$^+$ ILCs. As microbiota induces the generation of RORγt$^+$ T_H17 cells [34], our data indicate that microbiota represses IL-22 production by RORγt$^+$ ILCs both through IL-25 and adaptive immunity. Of note, adaptive immunity was not required for the IL-25-mediated repression of IL-22

production by RORγt$^+$ ILCs, as the administration of IL-25 efficiently repressed this activity in RAG-2-deficient mice (**Fig. 5c**).

Epithelial damage de-represses the activity of RORγt$^+$ ILCs

We next assessed the activity of RORγt$^+$ ILCs during intestinal inflammation. Epithelial damage was induced by oral exposure of *Rorc(γt)-Gfp*^{TG} mice to dextran sodium sulfate (DSS), which affects the colon, and to a lesser extent, the small intestine [42]. After two cycles of DSS administration followed by water, the expression of *Il22* was markedly increased in the intestine (**Fig. 6a**), as shown previously [16], concomitant with an increase in *Il23* and a sharp decrease in *Il25* expression by epithelial cells. The IL-22 production by RORγt$^+$ ILCs was increased to concentrations found in germfree mice (**Fig. 6b** and **3b**) and RORγt$^+$ ILCs expanded 3 to 4-fold (**Fig. 6c**). Thus, whereas microbiota and adaptive immunity repress the activity of RORγt$^+$ ILCs during steady state, epithelial damage that induces intestinal inflammation fully de-represses this activity and leads to an expansion of RORγt$^+$ ILCs. Remarkably, even in the context of intestinal inflammation, IL-25 repressed IL-22 production by RORγt$^+$ ILCs (**Fig. 6d**), demonstrating its dominant role in the regulation of RORγt$^+$ ILCs.

Finally, RORγt$^+$ ILCs were required for resistance to DSS-mediated colitis. Wild-type or RAG-2-deficient mice treated with IL-25 showed a significant increase in weight loss in response to DSS treatment, as well as a delayed recovery **(Fig. 7a and b)**. In that context, IL-25 also decreased the number of RORγt$^+$ T cells and repressed their production of IL-22 **(Supplementary Fig. 5)**. However, mice that lack RORγt$^+$ ILCs rapidly succumbed to DSS-mediated colitis [43], whereas RAG-2-deficient mice did not **(Fig. 7b)**. Of note, IL-25 efficiently repressed expression of *Reg3b* and *Reg3g* **(Fig. 4e)**, but only partially repressed IL-22 production by RORγt$^+$ ILCs **(Fig. 4d, 6d, 7c and 7d)**. In contrast, the absence of RORγt abolished expression of IL-22 **(Fig. 1b)** but not of *Reg3b* and *Reg3g* **(Fig. 1c)**, indicating that the IL-22 producing activity of RORγt$^+$ ILCs is involved in protection and recovery from DSS-mediated epithelial damage and colitis.

DISCUSSION

Lymphoid cells derived from common lymphoid progenitors (CLP) [44] include B and T cells, the hallmarks of adaptive immunity, and innate lymphoid cells (ILCs) including NK cells and LTi cells [45], which lack antigen receptors generated by somatic recombination. LTi cells, which express the nuclear hormone receptor RORγt [33], generate micro-inflammation at programmed sites in the fetus and adult intestine to induce the development of lymphoid tissues [33,35]. Recently, a new subset of RORγt$^+$ innate lymphoid cells (ILCs) has been described that resides mostly in the intestine. These cells express the pan-NK marker NKp46, but lack most other NK markers and are non-cytotoxic [23-27]. We now show that RORγt$^+$ ILCs produce most of intestinal IL-22 at steady state and markedly increase this activity during inflammation. RORγt$^+$ ILCs therefore play a critical role in intestinal homeostasis and defense, as IL-22 induces the production of anti-bacterial peptides by epithelial cells, is required for intestinal defense against bacterial and fungal pathogens [8-10,12,13] and is involved in protection of intestinal tissues from the effects of pathological inflammation, presumably through the induction of anti-apoptotic factors [15,16].

In marked contrast to RORγt$^+$ T cells [34], absolute numbers of RORγt$^+$ ILCs are unaffected in germfree mice, showing that the development of RORγt$^+$ ILCs is programmed [31]. This result may seem counter-intuitive, as RORγt is induced in developing T_H17 cells through the activation of Stat3 [46,47]. T_H17 cells are enriched in the intestine [36] where activators of Stat3, such as IL-6, IL-21 and IL-23 [48] abound, presumably in response to the large microbial community residing in the intestinal lumen. Microbiota also induces the generation of the NK1.1$^{lo/-}$ subset of RORγt$^+$ NKp46$^+$ cells [23,25,26]. Nevertheless, RORγt appears to be programmed in thymic subsets of γδ T cells [49] and iNKT cells [50], thus presumably in the absence of germs, and in LTi cells generated in the sterile environment of the fetus [28].

In addition to a programmed development, RORγt$^+$ ILCs show constitutive expression of IL-22, as well as of IL-17 by LTi cells. A role of IL-22 and IL-17 produced by LTi cells in the fetus remains to be elucidated, but appears evolutionary conserved in human [27]. After birth, the key role of IL-22 in intestinal homeostasis and defense, and more generally in mucosal immunity, is well documented [10,12,13]. It may therefore not come as a surprise that the immune system has evolved a constitutive pathway for the production of IL-22. However, as the size and structure of the intestinal symbiotic microbiota evolves with time, the amount of

IL-22 produced might need constant re-adjustments. In accordance with this view, we show that microbiota regulates IL-22-production by RORγt$^+$ ILCs. As components of the symbiotic microbiota, such as *Candidatus arthromitus*, also termed Segmented Filamentous Bacteria (SFB), have been shown to induce T_H17 cells [51,52], it will be important to assess whether SFB, and other species or phyla of symbiotic bacteria, regulate the activity of RORγt$^+$ ILCs.

We show that both microbiota and adaptive immunity repress the activity of RORγt$^+$ ILCs. It is possible that RORγt$^+$ T cells including T_H17 cells [36] repress RORγt$^+$ ILCs by competition for a common cytokine niche. As both type of cells express IL-17 and IL-22, they might be subject to similar regulation through a panel of cytokines that includes IL-6, IL-21, IL-23, IL-25, IL-27 [48]. Our data demonstrate the major role of IL-25 in the repression IL-22 production by RORγt$^+$ ILCs. In contrast, IL-23, a major inducer of IL-22 [17], does not regulate the production of IL-22 by RORγt$^+$ ILCs during homeostasis, and is not repressed by IL-25. The role of other T_H17 regulators on RORγt$^+$ ILCs remains to be assessed.

Microbiota appears to be a positive regulator of IL-22 produced by T_H17 cells, but a negative regulator of IL-22 produced by innate RORγt$^+$ cells. In addition, adaptive immunity represses both the number and IL-22-production by RORγt$^+$ ILCs. Microbiota might therefore repress the activity of RORγt$^+$ ILCs through both IL-25 and adaptive immunity. From the point of view of the host, RORγt$^+$ ILCs preempt colonization of the intestine by symbiotic microbiota, whereas adaptive immunity reacts to this colonization and regulates the preemptive innate immunity. This complex regulatory network probably reflects the superposition of adaptive immunity over the more ancient innate preemptive system, and shows the subtle interplay between microbiota and the different forces of the vertebrate immune system to maintain intestinal homeostasis.

Finally, a rupture in intestinal homeostasis is induced by epithelial damage (achieved here by the administration of DSS) that provokes a strong inflammatory reaction to contain the breaching symbiotic microbiota [53]. In that highly challenging context, both T_H17 [36] and RORγt$^+$ ILCs expand, and IL-22 production is highest. Thus, whereas during steady state, microbiota, T_H17 and RORγt$^+$ ILCs are controlled by a complex regulatory network, during tissue damage and consequent inflammation, both adaptive and innate RORγt$^+$ cells add up production of IL-22 to force a return to homeostasis. However, such situations are potentially dangerous to the host, as the pro-inflammatory activity of T_H17 cells and RORγt$^+$ ILCs may expand beyond control and induce inflammatory pathology [54-56].

ACKNOWLEDGEMENTS

We thank the members of the DTL lab for discussions and critical reading of the manuscript, Lucette Polomack for technical assistance, and José Perez and Eddie Maranghi for excellent work on germfree mice. We also thank B. Ryffel for providing us with p19-deficient mice. This study was supported by the Institut Pasteur, grants from the Mairie de Paris, the Agence Nationale de la Recherche, and an Excellence Grant from the European Commission. M.L. was supported by the Deutsche Forschungsgemeinschaft and the Schlumberger Foundation. The authors have no competing financial interests.

AUTHOR CONTRIBUTIONS

S.S. and G.E. designed the study and wrote the manuscript; S.S. did most of the experimental work; M.L. contributed to the analysis of T cells and DSS-mediated colitis; N.S.-T. contributed to the analysis of $NKp46^{+}$ ILCs; S.D. performed laser capture microdissection; M.B. generated germfree mice; M.K. and D.C. generated and provided IL-25-deficient mice; J.P.D.S contributed to data analysis and manuscript writing.

COMPETING FINANCIAL INTERESTS

The authors declare no competing financial interests.

LEGENDS TO FIGURES

Figure 1 RORγt$^+$ ILCs are the major producer of IL-22 in the intestine. (**a**) Small intestinal lamina propria leukocytes (SI-LPL) from E.15, 2 weeks and 8 weeks old *Rorc(γt)-Gfp*^{TG} mice were analyzed by flow cytometry. The production of IL-22 was assessed by intracellular cytokine staining after 3 hours of stimulation with IL-23 *ex vivo*, and IL-22$^+$ RORγt$^+$ cells were further analyzed for the expression of CD3ε and CD4. Numbers indicate percent cells per quadrant. The data are representative of three independent experiments. (**b**) Expression of transcripts for IL-22 in the terminal ileum of 8 weeks old wild type, RAG2-deficient, RORγt-deficient and RAG2/RORγt-double deficient mice. Data are mean of qPCR triplicates and n = 4 mice per group. NS, statistically not significant; unpaired t-test. (**c**) Expression of transcripts for RegIIIβ and RegIIIγ by epithelial cells from 8 weeks old wild type, RAG2-deficient and RORγt-deficient mice. Data are mean of qPCR triplicates and n = 4 mice per group. NS, statistically not significant; unpaired t-test. (**d**) RORγt$^+$ ILCs (GFP$^+$ CD3ε$^-$ cells) were analyzed for their surface expressions of CD4 and NKp46. Data are representative of at least n = 8 individual mice.

Figure 2 The production of pro-inflammatory cytokines by RORγt$^+$ ILCs. SI-LPL from E15, 2 weeks and 8 weeks old *Rorc(γt)-Gfp*^{TG} mice were analyzed by real-time qPCR for the expression of transcripts and by flow cytometry for the expression of protein for (**a**) IL-22, (**b**) IL-17, (**c**) LTα and IFNγ. qPCR data are mean of three independent experiments ± S.E.M.; $^*P < 0.05$, NS, statistically not significant, unpaired t-test. ND, non-detected. The data are representative of five independent experiments. In histograms, numbers are mean of n = 10 mice ± S.E.M percentages of IL-22$^+$ or IL-17$^+$ cells compared to isotype controls (shown in blue). Cells were stimulated for 3 hours *ex vivo* with rIL-23 or PMA/ionomycin, respectively.

Figure 3 Microbiota represses the production of IL-22 by RORγt$^+$ ILCs. (**a**) Absolute numbers of RORγt$^+$ ILCs and CD4$^+$ T cells in SI-LPL from 10 weeks old germ free (GF) mice as compared with age matched specific pathogen free (SPF) mice (left panel), and in 6 weeks old antibiotic-treated mice as compared to non-treated controls (right panel). The histograms are compilations of data obtained from n = 4 mice per group. $^*P < 0.05$, NS, statistically not significant, unpaired t-test. (**b**) RORγt$^+$ILCs and CD4$^+$ T cells from 8 weeks old SPF, antiobiotic (Abx)-treated or GF *Rorc(γt)-Gfp*^{TG} mice were analyzed for the expression of

transcripts and protein for IL-22. Protein expression was analyzed after 3 hr stimulation *ex vivo* with IL-23. Data are mean of qPCR triplicates and n = 3 mice per group. In histograms, numbers indicate the mean ± S.E.M percentage of IL-22$^+$ cells obtained from n = 4 mice per group. (**c**) Transcripts for IL-17 in RORγt$^+$ILCs and CD4$^+$ T cells from SPF or GF *Rorc(γt)-Gfp*^{TG} mice.

Figure 4 Microbiota represses the activity of RORγt$^+$ ILCs through IL-25. (**a**) Epithelial cells were isolated by laser capture microdissection from the terminal ileum of 6 weeks old SPF or GF C57BL/6 mice, and from 2 weeks or 8 weeks old SPF C57BL/6 mice, and analyzed for the expression of transcripts for IL-25. Data are mean of qPCR triplicates and n = 2 mice per group. (**b**) Absolute numbers of RORγt$^+$ ILCs in SI-LPL of 8 weeks old wild-type and IL-25-deficient (IL-25KO) mice. Data are the mean of qPCR triplicates and n = 3 mice per group. (**c**) Production of transcripts and protein for IL-22 by RORγt$^+$ ILCs isolated from 8 weeks old wild-type or IL-25-deficient mice. Protein expression was analyzed after 3 hr stimulation *ex vivo* with IL-23. FACS data are representative of two independent experiments and the numbers indicate mean ± S.E.M percentage of IL-22+ cells obtained from n = 4 mice. (**d**) IL-22 production by RORγt$^+$ILCs in 6 weeks-old *Rorc(γt)-Gfp*^{TG} mice treated with rIL-25 or PBS. Data are representative of three independent experiment and the numbers indicate the mean ± S.E.M percentage of IL-22$^+$ cells obtained from n = 6 mice. (**e**) Expression of transcripts for RegIIIβ and RegIIIγ by epithelial cells from 6 weeks old mice treated with rIL-25 or PBS. (**f**) Expression of IL-17BR (IL-25R) by lineage$^-$ (CD5$^-$ B220$^-$ CD11b$^-$ Gr-1$^-$ Ter119$^-$) cells from 6 weeks old *Rorc(γt)-Gfp*^{TG} mice and CD3ε$^-$ CD19$^-$ SI-LPL from wild-type mice treated with rIL-25 or PBS. Histology shows a cryptopatch in sections from the terminal ileum of 4 weeks-old *Rorc(γt)-Gfp*^{TG} mice. Bar, 50μm. (**g**) RORγt$^+$ ILCs were isolated from 4 weeks-old *Rorc(γt)-Gfp*^{TG} mice and cultured in the presence of rIL-25 with or without IL-17BR$^+$CD11c$^+$ cells sorted from SI-LPL of 4 weeks-old wild type mice. (**h**) RORγt$^+$ ILCs were cultured in the presence of PBS (left) or rIL-25, with IL-17BR$^+$CD11c$^+$ cells in the same well (middle) or separated by a transwell of 0.4 μm pore size (right). After 3-days, RORγt$^+$ ILCs were re-sorted and *Il22* gene expression was analyzed by qPCR. Shown are mean of results obtained from triplicate wells. Data are compilations of two independent experiments. $^*P < 0.05$, NS, statistically not significant, unpaired *t*-test.

Figure 5 Adaptive immunity represses the activity of RORγt$^+$ ILCs. (**a**) SI-LPLs from 6 weeks old wild-type or RAG2-deficient *Rorc(γt)-Gfp*^{TG} mice were analyzed for intracellular IL-22 expression after 3 hr stimulation *ex vivo* with IL-23. Data are representative of three independent experiments, and the numbers indicate mean ± S.E.M percentage of IL-22$^+$ cells obtained from n = 6 mice. (**b**) Absolute numbers of RORγt$^+$ ILCs cells from 6 weeks old mice. Data shown are mean of n = 4 mice. (**c**) Expression of IL-22 by RORγt$^+$ ILCs from RAG2-deficient *Rorc(γt)-Gfp*^{TG} mice treated with rIL-25 or PBS. Data are representative of three independent experiments. Numbers indicate mean ± S.E.M percentage of IL-22$^+$ cells obtained from n = 6 mice. $^*P < 0.05$, NS, unpaired t-test.

Figure 6 Epithelial damage de-represses the activity of RORγt$^+$ ILCs. (**a**) Expression of transcripts for IL-22, IL-23 and IL-25 in total terminal ileum or microdissected epithelial cells from terminal ileum of mice treated with water or DSS. Data are mean of qPCR triplicates and n = 2 mice per group. (**b**) Expression of transcripts and protein for IL-22 by RORγt$^+$ ILCs isolated from 8 weeks old *Rorc(γt)-Gfp*^{TG} mice treated with water or DSS. FACS data are representative of three independent experiments. Numbers indicate mean ± S.E.M percentage of IL-22$^+$ cells obtained from n = 6 mice. (**c**) Absolute numbers of RORγt$^+$ ILCs in SI-LPL of 8 weeks old control and DSS-treated mice. Data are mean of n = 3 mice per group. (**d**) Expression of IL-22 by RORγt$^+$ ILCs in 6 weeks old *Rorc(γt)-Gfp*^{TG} mice treated with DSS and injected daily with rIL-25 or PBS. FACS data are representative of two independent experiments. Numbers indicate mean ± S.E.M percentage of IL-22$^+$ cells obtained from n = 6 mice. $^*P < 0.05$, unpaired t-test. Data in histograms are representative of three independent experiments.

Figure 7 The activity of RORγt$^+$ ILCs is required for protection and recovery from colitis. (**a**) Body weight of C57BL/6 mice injected with rIL-25 or PBS, or of (**b**) RAG2/RORγt-double deficient mice, or RAG2-deficient mice injected with rIL-25 or PBS, and treated with DSS. Data are the mean ± S.E.M of n = 5 mice per group. $^*P < 0.05$, unpaired t-test. † indicates death of one IL-25-injected RAG-2-deficient mice at day 9. **(c)** Expression of IL-22 by RORγt$^+$ ILCs in 9 weeks old RAG-2-deficient mice injected with rIL-25 or PBS every two days, and treated with DSS. Cells were stimulated for 3 hours *ex vivo* with PMA/ionomycin. Numbers in histograms indicate mean ± S.E.M of n = 3 mice per group. **(d)** Absolute numbers of small intestinal lamina propria RORγt$^+$ILCs of RAG2-deficient mice injected with rIL-25

or PBS, and treated with DSS. The histograms are compilations of data obtained from $n = 3$ mice per group. $^{*}P < 0.05$, unpaired *t*-test.

METHODS

Mice

BAC-transgenic *Rorc(γt)-Gfp*^{TG} mice [36] were kept in specific pathogen-free conditions. RAG2-deficient mice were further crossed with *Rorc(γt)-Gfp*^{TG} mice. Germfree *Rorc(γt)-Gfp*^{TG} mice were obtained by aseptic caesarean section followed by the adoption of the caesarean-derived pups by germ-free foster mothers. Health monitoring tests were performed to verify that the germ-free colony was also free of parasites and of mouse specific viruses. IL-23- or IL-25-deficient mice were described previously [57,58]. All animal experiments were approved by the committee on animal experimentation of the Institute Pasteur and strictly followed French regulation on animal experimentation.

Mouse treatments

To eradicate the intestinal bacterial flora, *Rorc(γt)-Gfp*^{TG} mice were treated with a cocktail of antibiotics containing 5g/L Streptomycin, 1g/L Colistin, 1g/L Ampicillin and 2.5% Sucrose (Sigma Aldrich) in the drinking water starting one day before birth, and until analysis at day 42. Antibiotic treatment was renewed every week. To induce gut inflammation, Dextran sulfate sodium (DSS) salt (M.W.= 36.000-50.000; MP Biomedicals, France) was dissolved in the drinking water at a concentration of 2,5% (m/v). 6 weeks old mice were exposed to DSS for 7 days followed by a recovery period of 10 days without DSS [36]. This cycle was repeated twice. The mice were analyzed at the age of 9 weeks. To assess the function of IL-25 in vivo, recombinant mouse IL-25 (R&D systems) was administrated (0.5µg in 100 µL PBS i.p) every other day for 21 days to adult *Rorc(γt)-Gfp*^{TG} or RAG2-deficient *Rorc(γt)-Gfp*^{TG} mice. Recombinant mouse IL-23 (R&D systems) (0.5µg in 100 µL PBS i.p) and neutralizing polyclonal goat anti-IL-23p19 Ab (R&D Systems) was injected to RAG-2-deficient mice daily. Neutralizing anti-IL-23R Ab (clone 258010) (R&D Systems) (10µg in 100 µL PBS i.v) was injected daily to *Rorc(γt)-Gfp*^{TG} mice.

Isolation of cells and flow cytometry

To isolate mononuclear cells from the small intestinal lamina propria (SI-LPL), Peyer's pathes were first removed, gut fragments were cut open and then incubated in PBS (Ca/Mg free) containing 30mM EDTA for 30 min at 4^{o}C. Tissues were then washed with PBS by vigorous shaking for 3 cycles. Washed gut pieces were subsequently cut into 1mm pieces and

incubated at 37°C for 60 min in DMEM (Gibco) containing 1mg/ml collagenase D (Roche) and 1U/ml DNase 1 (Invitrogen). Every 10 minutes, tissues were washed with warm DMEM and re-incubated with fresh Collagenase and DNase containing medium. Supernatants obtained in each step were collected. Fetal or neonatal total intestine were isolated and cut into 1mm pieces, and then incubated at 37°C for 30 min in DMEM (Gibco) containing 1mg/ml collagenase D and 1U/ml DNase 1. Remaining intestinal fragments were collected and pressed through a 100-µm mesh, mixed with the collected supernatants, and resuspended in a 40% Percoll solution (GE Healthcare). Mononuclear cells were collected from the interphase between 80% and 40% Percoll solutions after spin at 1350 g for 20 min. To obtain intraepithelial leukocyte (IEL), epithelial fraction obtained after 30mM EDTA incubation was collected. The epithelium-containing cell pellets were re-suspended with 10% Bovine serum containing DMEM, incubated for 30 min at 37°C and leukocytes were isolated with 40%-80% Percoll gradient. To obtain single cells from the lymph node and the spleen, organs were cut into 5mm pieces and incubated at 37°C for 30 min in DMEM containing 1mg/ml collagenase D and 1U/ml DNase 1 and then pressed through a 100-µm mesh. All cells were first preincubated with mAb 2.4G2 to block Fc γ receptors, and then washed and incubated with the indicated mAb conjugates for 40 min in a total volume of 100 μl PBS containing 2mM EDTA and 2% bovine serum. Cells were analysed on FACSCanto I or FACSCanto II (BD Biosciences) and Flowjo software (Tristar). Cells were sorted with a FACS Aria (BD Biosciences) to a purity of 95-98%.

Antibodies

Purified polyclonal anti-GFP, Alexa Fluor® 488-conjugated anti-Rabbit, PE-Cy3-conjugated anti-Armenian Hamster antibodies and Alexa Fluor® 647-conjugated Streptavidin, were purchased from Invitrogen. Purified anti-B220 (RA3-6B2), PE-conjugated anti-CD11c (N418), anti-IL-22 (1H8PWSR), anti-CD117 (2B8), anti-NKp46 (29A1.4), anti-RORγt (AFKJS-9), $RatIgG_1$ isotype control (eBRG1); PerCP-conjugated Streptavidin; PerCP Cy5.5-conjugated anti-CD4 (RM4-5); PE-Cy7-conjugated Streptavidin, anti-CD19 (eBio1D3); APC-conjugated anti-CD127 (A7R34), anti-B220 (RA3-6B2), anti-IFNγ (XMG1.2), anti-CD11c (N418), anti-CD11b (M1/70), RatIgG1 isotype control; Pacific blue-conjugated anti-CD3ε (500A2); Alexa Fluor® 647-conjugated anti-IL-17 (eBio17B7), and APC-Alexa Fluor® 780 conjugated anti-CD3ε (17A2) and anti-CD117 (ACK2); Biotin-conjugated anti-

TRANCE (IK22/5) were purchased from e-Bioscience. Biotin-conjugated anti-NKp46 and anti-IL17BR were from R&D systems.

Cell stimulation and intracellular staining

To assess intracellular IL-17A, IL-22 and IFNγ, cells were stimulated for 3hr in DMEM containing 50 ng/ml Phorbol 12-Myristate 13-Acetate (PMA) and 500 ng/ml ionomycin (Sigma-Aldrich). For the last 1.5 hr, 10μg brefeldin A (Sigma-Aldrich) was added to the culture medium. In another setting to measure IL-22 expression, cells were stimulated with 40 ng/ml mouse recombinant IL-23 (R&D systems) for 3 hr. For the last 1.5 hr, 10μg brefeldin A (Sigma-Aldrich) was added to the culture medium. After surface staining for c-kit (CD117), CD4, NKp46, IL-7Rα (CD127) and/or CD3ε, stimulated cells were fixed with 4% PFA (Sigma-Aldrich) and permeabilized with 1% saponin (Sigma-Aldrich) followed by intracellular cytokine staining. To detect intracellular RORγt, the Foxp3-staining buffer set (e-Bioscience) was used for fixation and permeabilization of the cells.

Cultures of RORγt$^+$ ILCs

Total RORγt (GFP)$^+$ ILCs were sorted by flow cytometry from SI-LPL of 4 weeks-old *Rorc(γt)-Egfp*^{TG} mice. 2000 ILCs were re-suspended in culture medium and seeded into flat bottom 96-well plates coated with OP9 stroma cells. Culture medium was OPTI MEM containing 10% FCS, β2-Melcaptoethanol, ampicilin and streptomycin, in the presence of 20ng/ml mouse rIL-7, 20ng/ml mouse rSCF (PeproTec) and 20ng/mL mouse rIL-25 (R&D systems) in 24 well plates or in transwell plates with 12 mm diameter inserts (0.4 μm pore size) (Corning). After 3 days of culture, ILCs and OP9 stroma cells were dissociated with Cell Dissociation Buffer (GIBCO) and RORγt$^+$ ILCs were sorted by FACS ARIA. In another setting, IL-25R (IL17BR)$^+$CD11c$^+$ cells were sorted from SI-LPL of 4 weeks-old wild type (littermate of *Rorc(γt)-Egfp*^{TG}) mice, and 2000 IL-25R$^+$CD11c$^+$ cells were cultured with 2000 ILCs.

ELISA

Tissue fragments 1 cm in size were pepared from the terminal ileum of IL-25-treated or non-treated C57BL/6 wild type mice, washed with sterile PBS three times and cultured with 1 ml of serum free DMEM medium for 24hrs. Supernatants were centrifuged and assessed for IL-23a protein by ELISA using the Single Analyte ELISAssay^{TM} Kit (SABiosciences).

RNA isolation and qPCR

To perform gene expression analysis, whole tissue from the middle and terminal part of the colon was immediately frozen in liquid nitrogen upon animal sacrifice. Tissue was homogenized using Ultra Turrax T8 (IKA-Werke, Germany) in TRIZOL regent and total RNA was purified according to the manufacture's protocol (Invitrogen). RNA was subjected to DNase I digestion and additional purification using RNeasy Mini kit (Quiagen). In the case of sorted cells and epithelial cells isolated by laser capture microdissection, mRNA was linearly amplified using the Message Booster kit for quantitative RT-PCR (Epicentre Biotechnologies). RNA was transcribed into cDNA using Superscipt III reverse transcriptase (Invitrogen) according to the manufacture's protocol. Quantitative real time PCR was performed using RT^2 qPCR Primer sets or the Mouse Autoimmunity & Inflammation PCR Array and the RT^2 SYBR-Green master mix (SABiosciences) on a PTC-200 thermocycler equipped with a Chromo4 detector (Bio-Rad Laboratories). Data was analysed using Opticon Monitor software (Bio-Rad Laboratories). CT values were normalized to the mean CT values obtained for the two house keeping genes *Hsp90* and *Gapdh*. For the analysis of ILCs derived from *Il25*$^{-/-}$ mice, CT values were normalized to *Rorc* gene expression. All the primers for quantitative PCR of following genes were purchaced from SABiosciences: *Hsp90* (NM_008302), *Gapdh* (NM_008084), *Lta* (NM_010735), *Trance* (NM_011613), *Il22* (NM_016971), *Il17a* (NM_010552), *Ifng* (NM_145856), *Il23a* (NM_031252), *Il25* (NM_080729), *Reg3b* (NM_011036), *Reg3g* (NM_011260), *Rorc* (NM_011281) and *Il23r* (NM_144548).

Immunofluorescence histology

Tissues were washed and fixed overnight at 4°C in a fresh solution of 4% paraformaldehyde (Sigma-Aldrich) in PBS. The samples were then washed for 1 d in PBS, incubated in a solution of 30% sucrose (Sigma-Aldrich) in PBS until the samples sank, embedded in OCT compound 4583 (Sakura Finetek), frozen in a bath of isopentane cooled with liquid nitrogen, and stocked at -80°C. Frozen blocs were cut at 8-μm thickness, and sections were collected onto Superfrost/Plus slides (VWR). Slides were dried for 1 h and processed for staining or stocked at -80°C. For staining, slides were first hydrated in PBS-XG (PBS containing 0.1% Triton X-100 and 1% normal goat serum; Sigma-Aldrich) for 5 min and blocked with 10% bovine serum in PBS-XG for 1 h at 20^{o} C. Endogenous biotin was blocked with a biotin blocking kit (Vector Laboratories). Slides were then incubated with primary polyclonal

antibody or conjugated mAb (in general 1/100) in PBS-XG overnight at 4°C, washed three times for 5 min with PBS-XG, incubated with secondary conjugated polyclonal antibody or streptavidin for 1 h at 20° C, washed once, incubated with DAPI (Sigma-Aldrich) for 5 min at 20° C, washed three times for 5 min, and mounted with Fluoromount-G (SouthernBiotech). Slides were examined under an AxioImager M1 fluorescence microscope (Carl Zeiss, Inc.) equipped with a CCD camera, and images were processed with AxioVision software (Carl Zeiss, Inc.).

Statistical analysis

A two-tailed Student's *t*-test was used for all statistical analysis.

REFERENCES

1. Backhed, F., Ley, R.E., Sonnenburg, J.L., Peterson, D.A. & Gordon, J.I. Host-bacterial mutualism in the human intestine. *Science* **307**, 1915-1920 (2005).
2. Duerkop, B.A., Vaishnava, S. & Hooper, L.V. Immune responses to the microbiota at the intestinal mucosal surface. *Immunity* **31**, 368-376 (2009).
3. Nagler-Anderson, C. Man the barrier! Strategic defences in the intestinal mucosa. *Nat Rev Immunol* **1**, 59-67 (2001).
4. Eberl, G. & Lochner, M. The development of intestinal lymphoid tissues at the interface of self and microbiota. *Mucosal Immunol* **2**, 478-485 (2009).
5. Round, J.L. & Mazmanian, S.K. The gut microbiota shapes intestinal immune responses during health and disease. *Nat Rev Immunol* **9**, 313-323 (2009).
6. Eberl, G. A new vision of immunity: homeostasis of the superorganism. *Mucosal Immunol* **3**, 450-460 (2010).
7. Brandl, K. *et al.* Vancomycin-resistant enterococci exploit antibiotic-induced innate immune deficits. *Nature* **455**, 804-807 (2008).
8. Wolk, K. *et al.* IL-22 increases the innate immunity of tissues. *Immunity* **21**, 241-254 (2004).
9. Wolk, K. *et al.* IL-22 regulates the expression of genes responsible for antimicrobial defense, cellular differentiation, and mobility in keratinocytes: a potential role in psoriasis. *Eur J Immunol* **36**, 1309-1323 (2006).
10. Zheng, Y. *et al.* Interleukin-22 mediates early host defense against attaching and effacing bacterial pathogens. *Nat Med* **14**, 282-289 (2008).
11. Sonnenberg, G.F., Monticelli, L.A., Elloso, M.M., Fouser, L.A. & Artis, D. CD4(+) Lymphoid Tissue-Inducer Cells Promote Innate Immunity in the Gut. *Immunity* (in press).
12. Aujla, S.J. *et al.* IL-22 mediates mucosal host defense against Gram-negative bacterial pneumonia. *Nat Med* **14**, 275-281 (2008).
13. De Luca, A. *et al.* IL-22 defines a novel immune pathway of antifungal resistance. *Mucosal Immunol* **3**, 361-373 (2010).
14. Pan, H., Hong, F., Radaeva, S. & Gao, B. Hydrodynamic gene delivery of interleukin-22 protects the mouse liver from concanavalin A-, carbon tetrachloride-, and Fas ligand-induced injury via activation of STAT3. *Cell Mol Immunol* **1**, 43-49 (2004).

15. Zenewicz, L.A. *et al.* Interleukin-22 but not interleukin-17 provides protection to hepatocytes during acute liver inflammation. *Immunity* **27**, 647-659 (2007).
16. Zenewicz, L.A. *et al.* Innate and adaptive interleukin-22 protects mice from inflammatory bowel disease. *Immunity* **29**, 947-957 (2008).
17. Kastelein, R.A., Hunter, C.A. & Cua, D.J. Discovery and biology of IL-23 and IL-27: related but functionally distinct regulators of inflammation. *Annu Rev Immunol* **25**, 221-242 (2007).
18. Zheng, Y. *et al.* Interleukin-22, a T(H)17 cytokine, mediates IL-23-induced dermal inflammation and acanthosis. *Nature* **445**, 648-651 (2007).
19. Kreymborg, K. *et al.* IL-22 is expressed by Th17 cells in an IL-23-dependent fashion, but not required for the development of autoimmune encephalomyelitis. *J Immunol* **179**, 8098-8104 (2007).
20. Liang, S.C. *et al.* Interleukin (IL)-22 and IL-17 are coexpressed by Th17 cells and cooperatively enhance expression of antimicrobial peptides. *J Exp Med* **203**, 2271-2279 (2006).
21. Wolk, K., Kunz, S., Asadullah, K. & Sabat, R. Cutting edge: immune cells as sources and targets of the IL-10 family members? *J Immunol* **168**, 5397-5402 (2002).
22. Spits, H. & Di Santo, J.P. The expanding family of innate lymphoid cells: regulators and effectors of immunity and tissue remodeling. *Nat Immunol* **12**, 21-27 (2011).
23. Satoh-Takayama, N. *et al.* Microbial flora drives interleukin 22 production in intestinal NKp46+ cells that provide innate mucosal immune defense. *Immunity* **29**, 958-970 (2008).
24. Cella, M. *et al.* A human natural killer cell subset provides an innate source of IL-22 for mucosal immunity. *Nature* **457**, 722-725 (2009).
25. Sanos, S.L. *et al.* RORgammat and commensal microflora are required for the differentiation of mucosal interleukin 22-producing NKp46+ cells. *Nat Immunol* **10**, 83-91 (2009).
26. Luci, C. *et al.* Influence of the transcription factor RORgammat on the development of NKp46+ cell populations in gut and skin. *Nat Immunol* **10**, 75-82 (2009).
27. Cupedo, T. *et al.* Human fetal lymphoid tissue-inducer cells are interleukin 17-producing precursors to RORC+ CD127+ natural killer-like cells. *Nat Immunol* **10**, 66-74 (2009).
28. Mebius, R.E., Rennert, P. & Weissman, I.L. Developing lymph nodes collect $CD4^+CD3^-LT\beta^+$ cells that can differentiate to APC, NK cells, and follicular cells but not T or B cells. *Immunity* **7**, 493-504 (1997).

29. Eberl, G. & Littman, D.R. Thymic origin of intestinal αβ T cells revealed by fate mapping of RORγt^{+} cells. *Science* **305**, 248-251 (2004).
30. Takatori, H. *et al.* Lymphoid tissue inducer-like cells are an innate source of IL-17 and IL-22. *J Exp Med* **206**, 35-41 (2009).
31. Sawa, S. *et al.* Lineage relationship analysis of ROR γ t+ innate lymphoid cells. *Science* **330**, 665-669 (2010).
32. Ivanov, II *et al.* The orphan nuclear receptor RORγt directs the differentiation program of proinflammatory IL-17^{+} T helper cells. *Cell* **126**, 1121-1133 (2006).
33. Eberl, G. *et al.* An essential function for the nuclear receptor ROR γ t in the generation of fetal lymphoid tissue inducer cells. *Nat Immunol* **5**, 64-73 (2004).
34. Ivanov, II *et al.* Specific microbiota direct the differentiation of IL-17-producing T-helper cells in the mucosa of the small intestine. *Cell Host Microbe* **4**, 337-349 (2008).
35. Bouskra, D. *et al.* Lymphoid tissue genesis induced by commensals through NOD1 regulates intestinal homeostasis. *Nature* **456**, 507-510 (2008).
36. Lochner, M. *et al.* In vivo equilibrium of proinflammatory IL-17+ and regulatory IL-10+ Foxp3+ ROR γ t+ T cells. *J Exp Med* **205**, 1381-1393 (2008).
37. Yoshida, H. *et al.* IL-7 receptor α^{+} CD3^{-} cells in the embryonic intestine induces the organizing center of Peyer's patches. *Int Immunol* **11**, 643-655 (1999).
38. Mebius, R.E. Organogenesis of lymphoid tissues. *Nat Rev Immunol* **3**, 292-303 (2003).
39. Zaph, C. *et al.* Commensal-dependent expression of IL-25 regulates the IL-23-IL-17 axis in the intestine. *J Exp Med* **205**, 2191-2198 (2008).
40. Neill, D.R. *et al.* Nuocytes represent a new innate effector leukocyte that mediates type-2 immunity. *Nature* **464**, 1367-1370 (2010).
41. Moro, K. *et al.* Innate production of T(H)2 cytokines by adipose tissue-associated c-Kit(+)Sca-1(+) lymphoid cells. *Nature* **463**, 540-544 (2009).
42. Geier, M.S., Smith, C.L., Butler, R.N. & Howarth, G.S. Small-intestinal manifestations of dextran sulfate sodium consumption in rats and assessment of the effects of Lactobacillus fermentum BR11. *Dig Dis Sci* **54**, 1222-1228 (2009).
43. Lochner, M. *et al.* Microbiota-induced tertiary lymphoid tissues aggravate inflammatory disease in the absence of ROR γ t and LTi cells. *J Exp Med* **208**, 125-134. (2011).
44. Kondo, M. *et al.* Biology of hematopoietic stem cells and progenitors: implications for clinical application. *Annu Rev Immunol* **21**, 759-806 (2003).

45. Eberl, G. Immunology: Close encounters of the second type. *Nature* **464**, 1285-1286 (2010).
46. Harris, T.J. *et al.* Cutting edge: An in vivo requirement for STAT3 signaling in TH17 development and TH17-dependent autoimmunity. *J Immunol* **179**, 4313-4317 (2007).
47. Mathur, A.N. *et al.* Stat3 and Stat4 direct development of IL-17-secreting Th cells. *J Immunol* **178**, 4901-4907 (2007).
48. Dong, C. TH17 cells in development: an updated view of their molecular identity and genetic programming. *Nat Rev Immunol* **8**, 337-348 (2008).
49. Jensen, K.D. *et al.* Thymic selection determines gammadelta T cell effector fate: antigen-naive cells make interleukin-17 and antigen-experienced cells make interferon gamma. *Immunity* **29**, 90-100 (2008).
50. Michel, M.L. *et al.* Critical role of ROR-gammat in a new thymic pathway leading to IL-17-producing invariant NKT cell differentiation. *Proc Natl Acad Sci U S A* **105**, 19845-19850 (2008).
51. Gaboriau-Routhiau, V. *et al.* The key role of segmented filamentous bacteria in the coordinated maturation of gut helper T cell responses. *Immunity* **31**, 677-689 (2009).
52. Ivanov, I.I. *et al.* Induction of Intestinal Th17 Cells by Segmented Filamentous Bacteria. *Cell* **139**, 485-498 (2009).
53. Hans, W., Scholmerich, J., Gross, V. & Falk, W. The role of the resident intestinal flora in acute and chronic dextran sulfate sodium-induced colitis in mice. *Eur J Gastroenterol Hepatol* **12**, 267-273 (2000).
54. Buonocore, S. *et al.* Innate lymphoid cells drive interleukin-23-dependent innate intestinal pathology. *Nature* **464**, 1371-1375 (2010).
55. Zenewicz, L.A., Antov, A. & Flavell, R.A. CD4 T-cell differentiation and inflammatory bowel disease. *Trends Mol Med* **15**, 199-207 (2009).
56. Sarra, M., Pallone, F., Macdonald, T.T. & Monteleone, G. IL-23/IL-17 axis in IBD. *Inflamm Bowel Dis* (2010).
57. Cua, D.J. *et al.* Interleukin-23 rather than interleukin-12 is the critical cytokine for autoimmune inflammation of the brain. *Nature* **421**, 744-748 (2003).
58. Kleinschek, M.A. *et al.* IL-25 regulates Th17 function in autoimmune inflammation. *J Exp Med* **204**, 161-170 (2007).

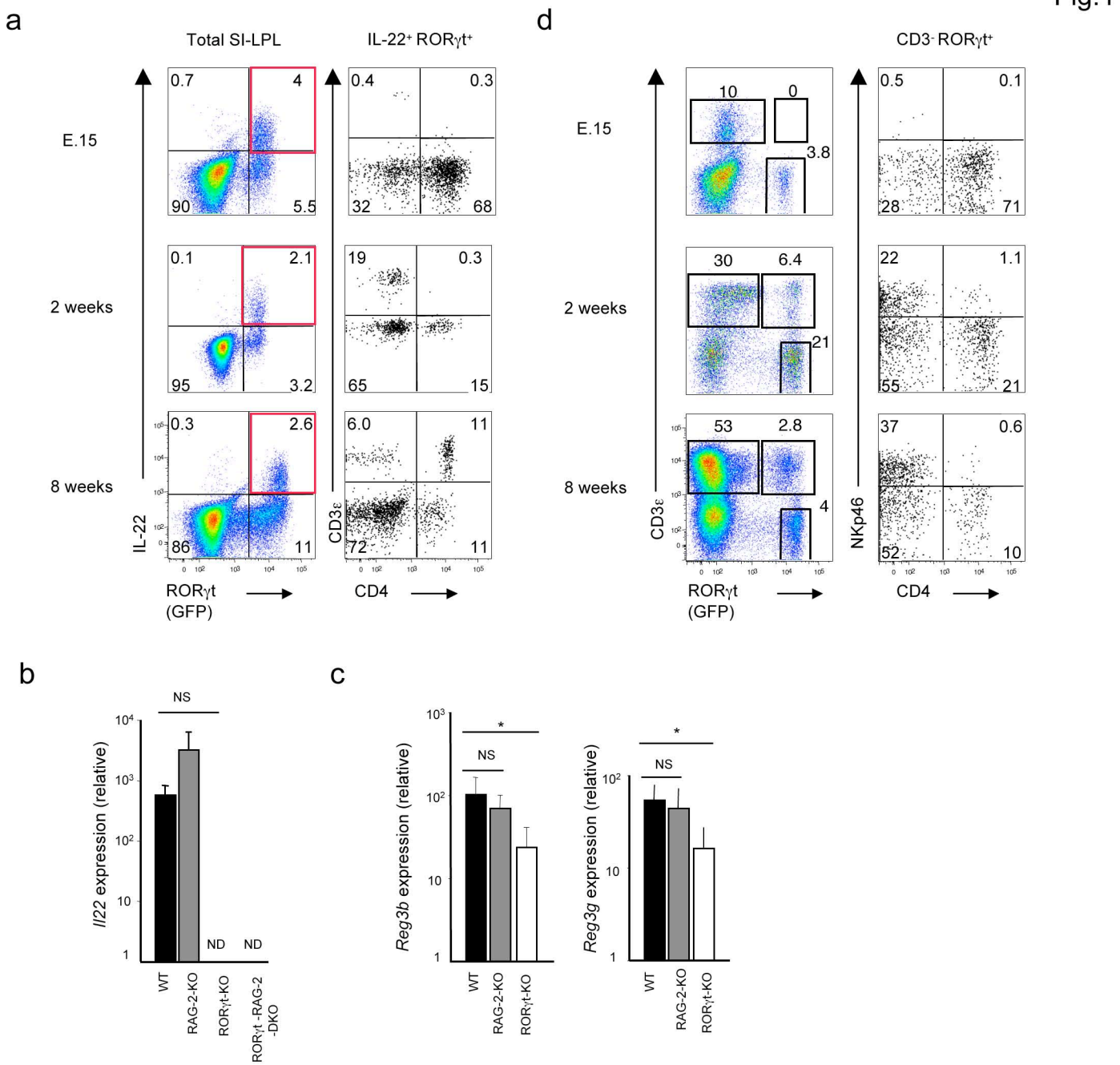
a
Total SI-LPL
IL-22+ RORγt+
E.15
2 weeks
8 weeks
0.7
4
90
5.5
0.4
0.3
32
68
0.1
2.1
95
3.2
19
0.3
65
15
0.3
2.6
86
11
6.0
11
72
11
IL-22
CD3ε
RORγt (GFP)
CD4
d
CD3- RORγt+
E.15
2 weeks
8 weeks
10
0
3.8
0.5
0.1
28
71
30
6.4
21
22
1.1
55
21
53
2.8
4
37
0.6
52
10
CD3ε
NKp46
RORγt (GFP)
CD4
b
Il22 expression (relative)
NS
ND
ND
WT
RAG-2-KO
RORγt-KO
RORγt -RAG-2 -DKO
c
Reg3b expression (relative)
Reg3g expression (relative)
*
NS
WT
RAG-2-KO
RORγt-KO

a

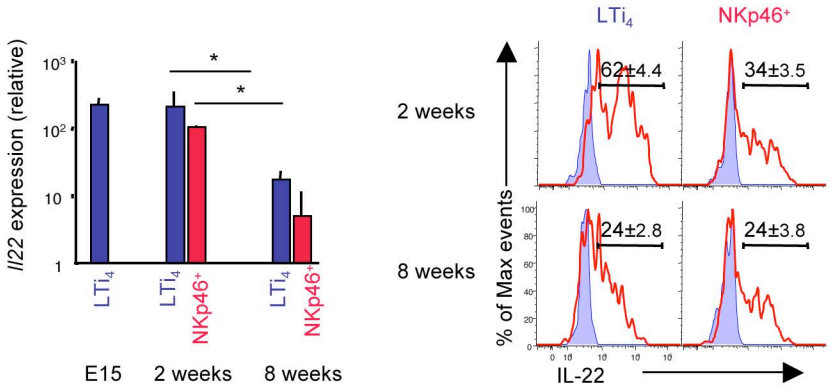
Il22 expression (relative)
LTi4
NKp46+
E15
2 weeks
8 weeks
2 weeks
8 weeks
62±4.4
34±3.5
24±2.8
24±3.8
% of Max events
IL-22

b

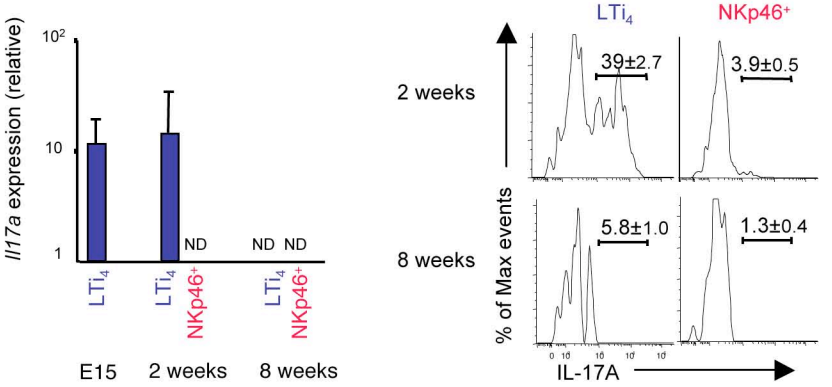
Il17a expression (relative)
ND
ND ND
LTi4
NKp46+
E15
2 weeks
8 weeks
2 weeks
8 weeks
39±2.7
3.9±0.5
5.8±1.0
1.3±0.4
% of Max events
IL-17A

c

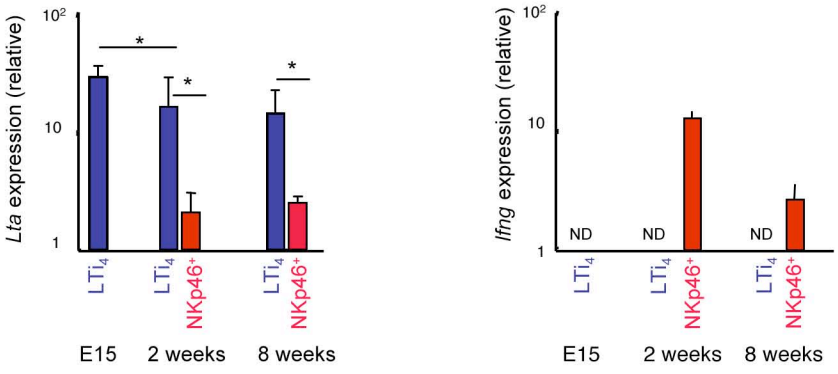
Lta expression (relative)
Ifng expression (relative)
ND
LTi4
NKp46+
E15
2 weeks
8 weeks

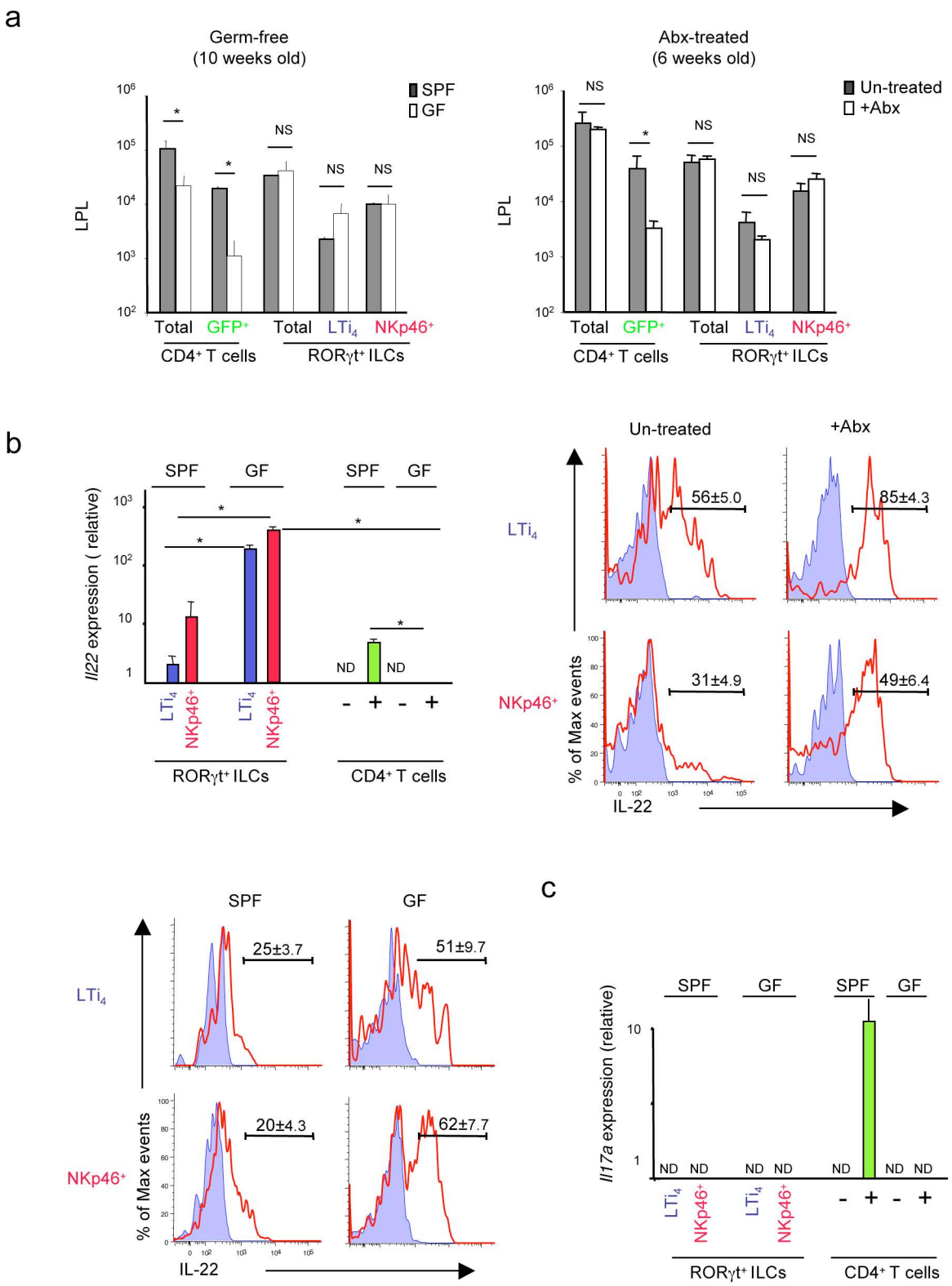
a
Germ-free
(10 weeks old)
SPF
GF
LPL
Total
GFP+
Total
LTi4
NKp46+
CD4+ T cells
RORγt+ ILCs
Abx-treated
(6 weeks old)
Un-treated
+Abx
b
Il22 expression (relative)
ND
LTi4
NKp46+
RORγt+ ILCs
CD4+ T cells
Un-treated
+Abx
56±5.0
85±4.3
31±4.9
49±6.4
% of Max events
IL-22
25±3.7
51±9.7
20±4.3
62±7.7
c
Il17a expression (relative)

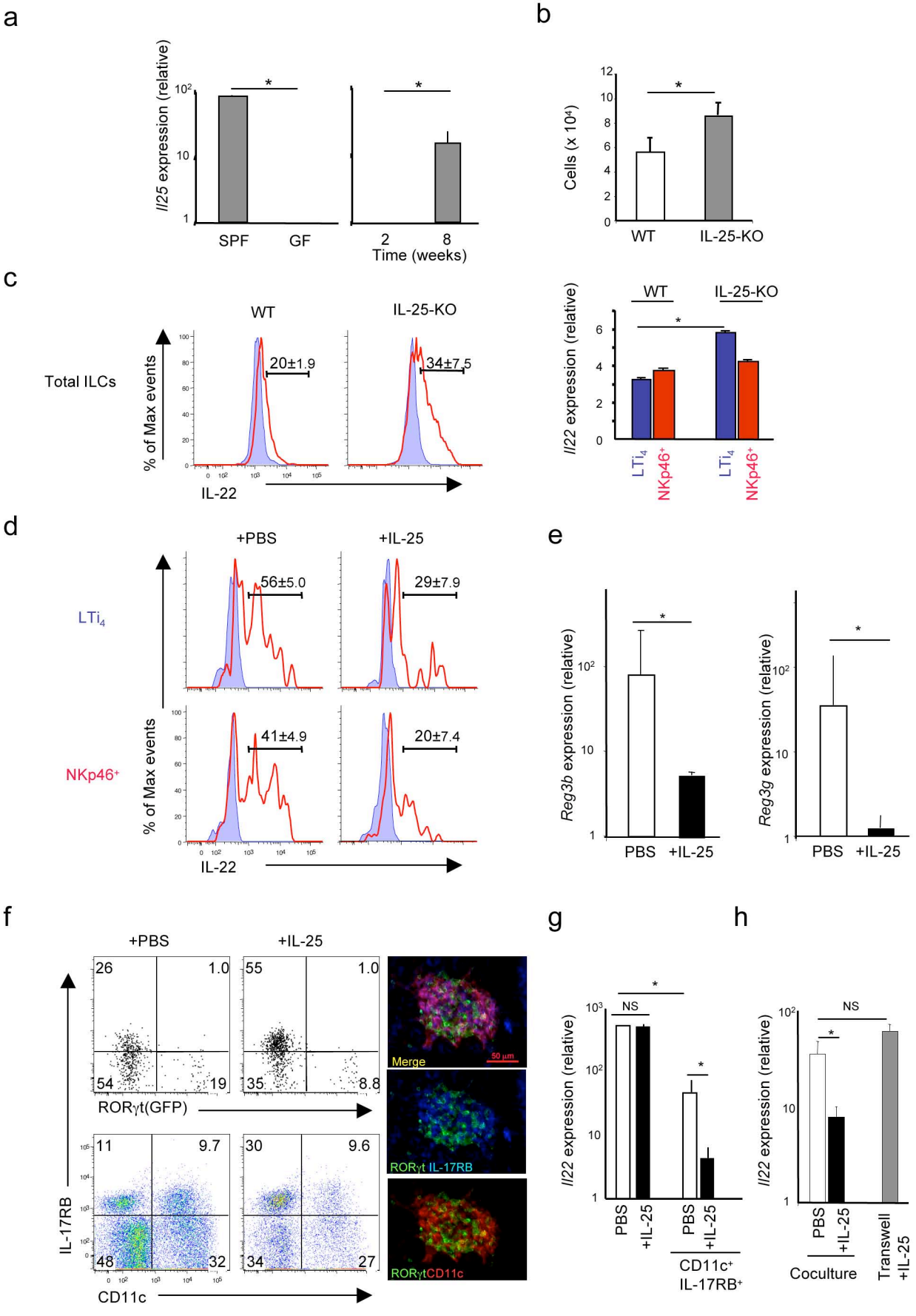
a
Il25 expression (relative)
SPF
GF
2
8
Time (weeks)
b
Cells (x 10⁴)
WT
IL-25-KO
c
Total ILCs
WT
IL-25-KO
20±1.9
34±7.5
% of Max events
IL-22
Il22 expression (relative)
LTi4
NKp46+
d
+PBS
+IL-25
LTi4
NKp46+
56±5.0
29±7.9
41±4.9
20±7.4
e
Reg3b expression (relative)
Reg3g expression (relative)
PBS
+IL-25
f
26
1.0
54
19
55
1.0
35
8.8
RORγt(GFP)
11
9.7
48
32
30
9.6
34
27
IL-17RB
CD11c
Merge
RORγt IL-17RB
RORγtCD11c
50 μm
g
NS
CD11c+
IL-17RB+
h
Coculture
Transwell
+IL-25

a

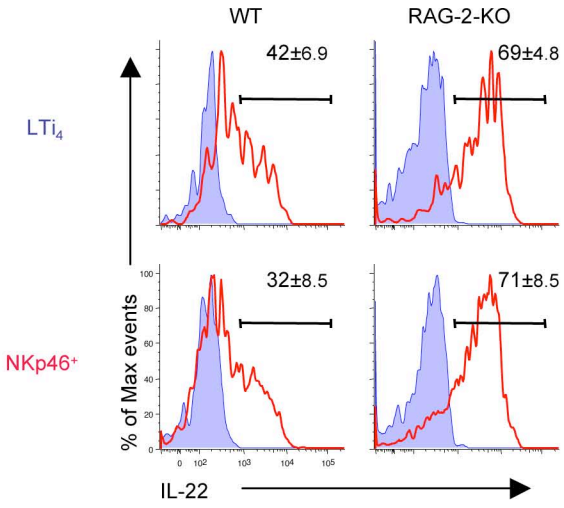
WT
RAG-2-KO
LTi4
NKp46+
42±6.9
69±4.8
32±8.5
71±8.5
% of Max events
IL-22

b

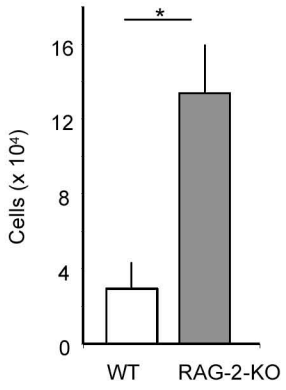
*
Cells (x 10⁴)
16
12
8
4
0
WT
RAG-2-KO

c

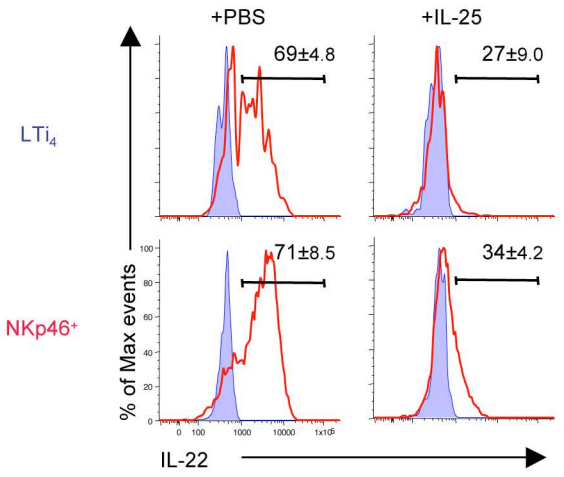
+PBS
+IL-25
LTi4
NKp46+
69±4.8
27±9.0
71±8.5
34±4.2
% of Max events
IL-22

a

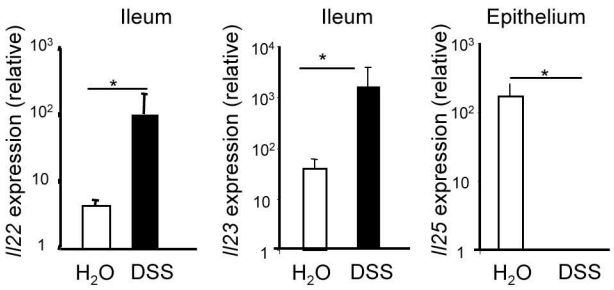
Ileum
Ileum
Epithelium
Il22 expression (relative)
Il23 expression (relative)
Il25 expression (relative)
H2O
DSS

c

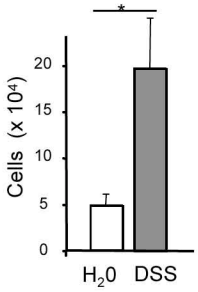
Cells (x 10⁴)
H20
DSS

b

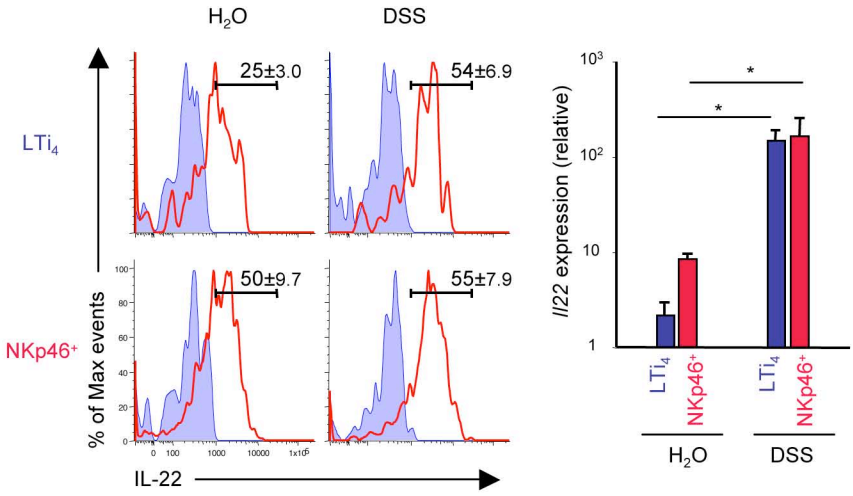
H2O
DSS
LTi4
NKp46+
25±3.0
54±6.9
50±9.7
55±7.9
% of Max events
IL-22
Il22 expression (relative)
LTi4
NKp46+
H2O
DSS

d

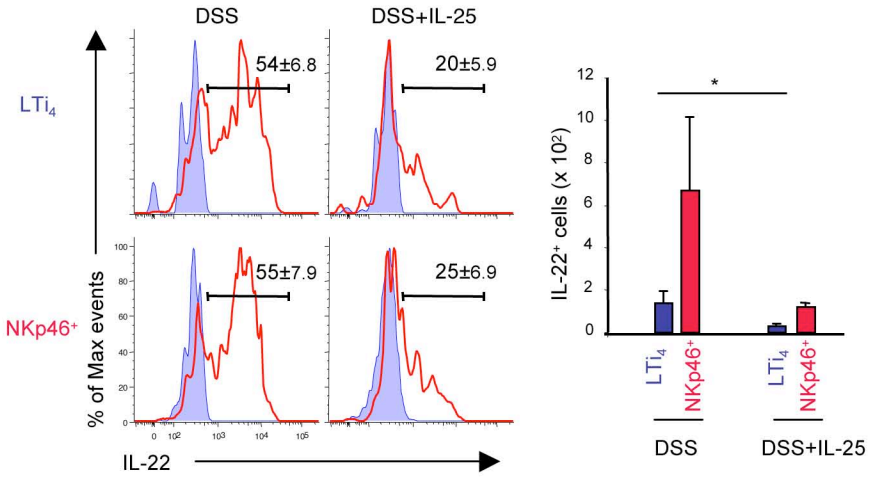
DSS
DSS+IL-25
LTi4
NKp46+
54±6.8
20±5.9
55±7.9
25±6.9
% of Max events
IL-22
IL-22+ cells (x 10²)
LTi4
NKp46+
DSS
DSS+IL-25

a

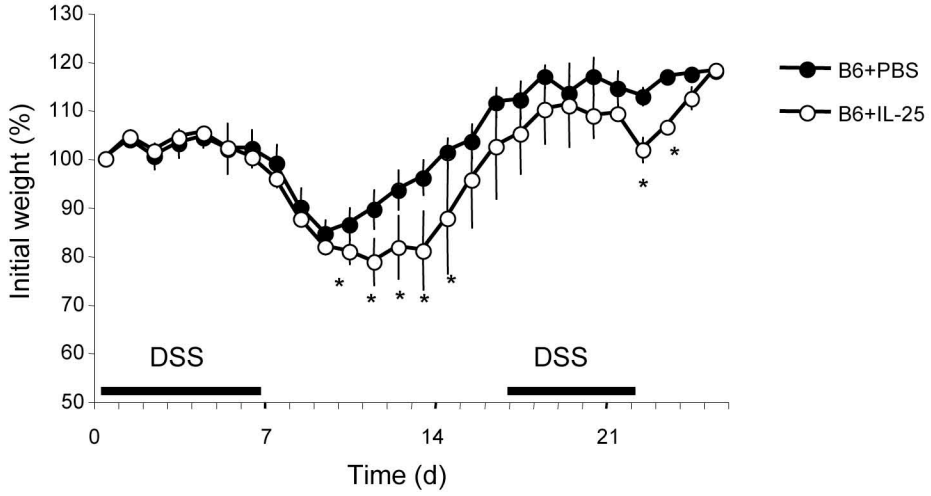
Initial weight (%)
130
120
110
100
90
80
70
60
50
DSS
DSS
0
7
14
21
Time (d)
B6+PBS
B6+IL-25

b

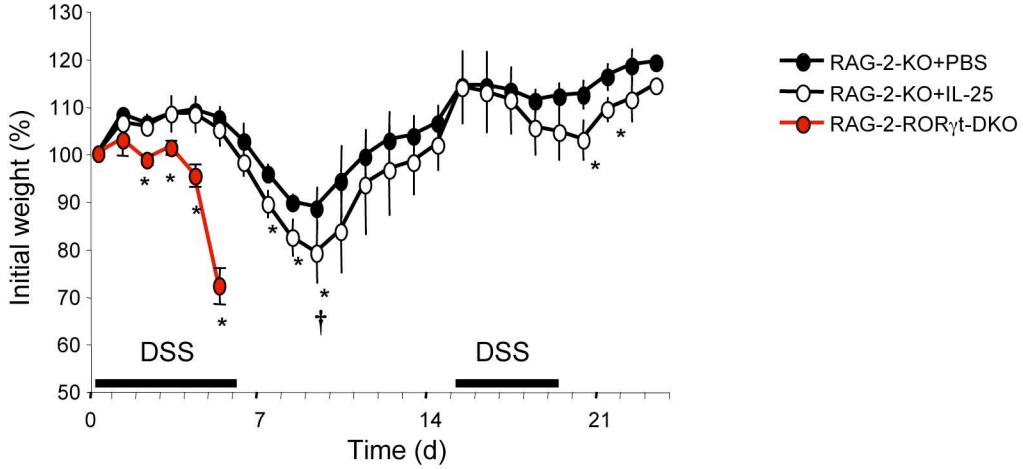
Initial weight (%)
130
120
110
100
90
80
70
60
50
DSS
DSS
0
7
14
21
Time (d)
RAG-2-KO+PBS
RAG-2-KO+IL-25
RAG-2-RORγt-DKO

c

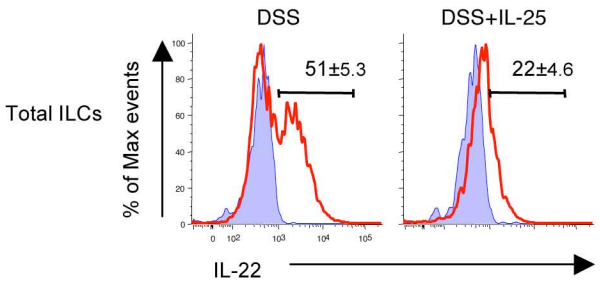
Total ILCs
% of Max events
DSS
DSS+IL-25
51±5.3
22±4.6
IL-22

d

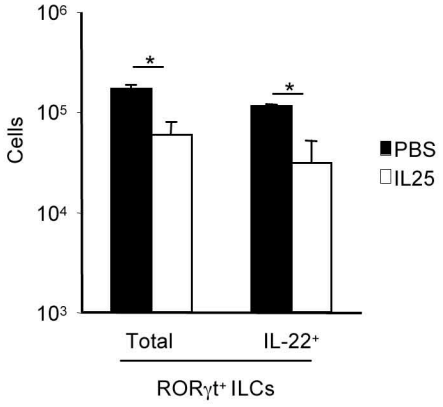
Cells
10⁶
10⁵
10⁴
10³
Total
IL-22⁺
RORγt⁺ ILCs
PBS
IL25